

Spectroscopic investigations of polycrystalline $\text{In}_x\text{Sb}_{20-x}\text{Ag}_{10}\text{Se}_{70}$ ($0 \leq x \leq 15$) multicomponent chalcogenides

RITA SHARMA¹, SHAVETA SHARMA¹, PRAVEEN KUMAR^{2,*}, RAVI CHANDER¹, R. THANGARAJ¹, M. MIAN¹

¹Semiconductors Laboratory, Department of Physics, GND University, Amritsar 143005, India

²Department of Physics, DAV University, Sarmastpur, Jalandhar-144012, India

The composition dependence of physical properties of chalcogenides has recently been studied for their phase change properties and energy conversion. In the present work, we report the structure, composition, optical and Raman spectroscopy results for bulk polycrystalline $\text{In}_x\text{Sb}_{20-x}\text{Ag}_{10}\text{Se}_{70}$ ($0 \leq x \leq 15$) samples. The phase quantification and composition have been studied by using XRD and EDX techniques. The alloy composition up to 5 at.% of indium resulted in crystallization of AgSbSe_2 , while further increase in In content favored the formation of another chalcopyrite AgInSe_2 phase yielding the solid solutions for this alloy system. A decrease in band gap up to $x = 5$ followed by its increase with an increase in indium concentration has been observed. The variations in shape and position of characteristic Raman bands has been used for understanding the structural modifications of the network with the variation in indium content.

Keywords: *chalcogenides; optical properties; Raman spectroscopy; XRD; XRD analysis; EDS*

© Wroclaw University of Technology.

1. Introduction

Chalcogenide glasses are very attractive because of their potential applications in passive and active solid state and optical devices, such as thermal imagining, memory switching, IR-photodetectors, photovoltaic systems and photoreceptors, etc. [1–6]. Se based chalcogenide alloys have emerged as a promising material due to their large potential applications in holography, e-beam recording and digital X-ray imaging [7, 8]. The reported physical characteristics have been improved by alloying Se with other elements. Sb_2Se_3 is an important photoconductive semiconductor which crystallizes in orthorhombic system [9, 10]. An addition of a third element usually affects the properties of chalcogenide semiconductors by creating compositional and configurational disorder in the material with respect to binary alloys [11]. Ag–Sb–Se is a narrow band gap p-type

semiconducting system which crystallizes to AgSbSe_2 with a cubic NaCl type structure [12]. Further, the incorporation of indium in Sb–Se system is expected to make it more suitable for reversible optical recording having less erase time [13]. However, an addition of Ag into the Sb–Se system increases its ionic conductivity and causes a large change in resistance with minute change in volume during crystallization to a single crystalline phase [14, 15]. The indium based chalcogenide alloys have also found applications as active material in non-volatile memory which uses the reversible phase transition of chalcogenide resistors [16]. The alloying of indium in the Ag–Sb–Se system might modify the lattice and optical properties what plays an important role in the fabrication of new devices. Thus, the present system is basically a quaternary or pseudo-ternary chalcogenide alloy system and is of interest for the development of new materials having improved efficiency, being less toxic and highly reproducible.

*E-mail: prafiziks@gmail.com

The chalcogenide glassy alloys have very useful properties which are strongly dependent on composition and various compositional thresholds viz. rigidity percolation threshold and chemical threshold for these network systems [17, 18]. Since the parent $Ag_{10}Sb_{20}Se_{70}$ ternary system has an average coordination number $\langle r \rangle = 2.20$ (<2.40), the system belongs to the floppy network [19]. Therefore, the isovalent substitution does not alter average coordination number of In–Sb–Ag–Se system. In this study, we have separated the effect of variation of $\langle r \rangle$ or composition from the nature of additive which is important for elaborating the further glassy systems. The crystalline structure of $In_xSb_{20-x}Ag_{10}Se_{70}$ ($0 \leq x \leq 15$) system has been investigated using optical and Raman spectroscopy. Modification of the structure caused by relative variation of In/Sb ratio or concentration of different cluster units with composition have been used for discussing the results.

2. Experimental

Bulk samples of $In_xSb_{20-x}Ag_{10}Se_{70}$ ($0 \leq x \leq 15$) system were prepared by conventional melt quenching technique. High purity (5N) elements in appropriate amounts were weighed and sealed in quartz ampoules under vacuum of $\sim 10^{-2}$ Pa. The ampoules were kept in a vertical furnace at 970 °C for 48 hours. Each ampoule was inverted at regular intervals of time to ensure a homogeneous sample and finally air quenched to get the bulk material. The quenched material was separated from the quartz ampoule by using HF + H_2O_2 for approximately 48 hours. The as-prepared bulk was further taken for characterization by using different techniques. The amorphous/crystalline phases in the as-prepared samples were studied by using X-ray diffractometer (D8 FOCUS, Bruker, Germany) with $CuK\alpha$ ($\lambda = 1.5405$ Å) line. The Raman spectra were studied by using an argon ion laser at a wavelength of 514 nm (Renishaw in via Reflex Micro Raman Spectrometer) and 2400 lines per mm diffraction grating having a suitable filter. Chemical composition was studied by EDX (Oxford Instrument, UK) equipped with FESEM (Supra 55, Carl Zeiss, Germany).

Diffuse reflectance measurements were carried out by using UV-Vis-NIR spectrophotometer (UV-3600, Shimadzu, Japan).

3. Results and discussion

3.1. Composition and crystalline phases

The elemental composition of each bulk sample was determined by energy dispersive X-ray spectroscopy (EDS) and the EDS spectra are shown in Fig. 1. The atomic percentages of all elements present in the bulk alloys are given in Table 1. These results suggest that the samples are nearly stoichiometric with those of the initial compositions used for the synthesis.

The structural analysis of devitrified glassy alloys and their phases is important for furthering the science of chalcogenide alloys. Fig. 2 shows the X-ray diffraction patterns of $In_xSb_{20-x}Ag_{10}Se_{70}$ chalcogenide alloys. The existence of sharp diffraction peaks for different phases in the multicomponent chalcogenide alloys reveals their polycrystalline nature. The crystalline phases are indexed to tetragonal phases of $AgSbSe_2$ (JCPDF Card No. 12-0379) and $AgInSe_2$ (JCPDF Card No. 75-0118) having a body centered lattice. The structural analysis of $Se_{70}Sb_{20}Ag_{10}$ reveals the devitrification of single phase $AgSbSe_2$ [12] without denomination of other phases due to their large intensity. The addition of small amount of indium additive ($x = 5$) results in a decrease in the intensity of diffraction peaks of $AgSbSe_2$ without forming new phases. However, further increase in x (10 at.%) favors the appearance of new diffraction peaks with increased intensity for $AgInSe_2$ phase, accompanied with peaks of decreased intensity for $AgSbSe_2$ phase.

Further addition of indium ($x = 15$) results in an increase in the $AgInSe_2$ phase and decrease in $AgSbSe_2$ phase.

3.2. Raman spectroscopy

Raman spectra yield valuable information about the dynamics and structure at the molecular level. The Raman spectra have been shown in Fig. 3. The Raman spectrum for the parent $Sb_{20}Ag_{10}Se_{70}$

Table 1. Compositions of as-prepared bulk $\text{In}_x\text{Sb}_{20-x}\text{Ag}_{10}\text{Se}_{70}$ ($0 \leq x \leq 15$) chalcogenide alloys obtained by using EDS spectroscopy.

x	at.%			
	Se	Sb	Ag	In
0	72.66	18.04	9.30	0.00
5	72.10	13.75	9.56	4.59
10	72.42	9.85	8.95	8.77
15	74.70	4.53	8.57	12.20

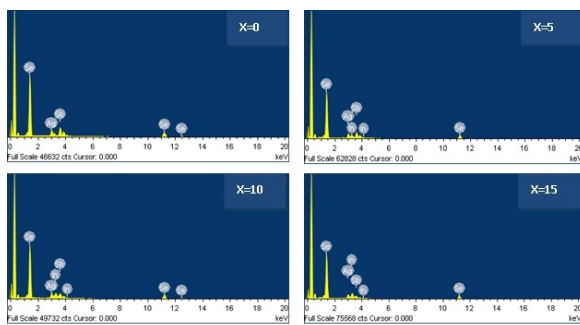


Fig. 1. EDS spectra of $\text{In}_x\text{Sb}_{20-x}\text{Ag}_{10}\text{Se}_{70}$ chalcogenide alloys.

chalcogenide alloy exhibits three dominant peaks at 82 cm^{-1} , 188 cm^{-1} and 252 cm^{-1} , and two weak bands at 117 cm^{-1} and 371 cm^{-1} . The Raman spectra of In–Ag–Sb–Se systems have been discussed by considering AgSbSe_2 and AgInSe_2 basic structural units. For simplifying the discussion, the R-value has been defined as a ratio of covalent bonding possibility of chalcogen atoms to the covalent bonding possibility of the non-chalcogen atoms [20]. The value of $R = 1$ represents the case of existence of only hetero-nuclear bonds in a given system which unequivocally indicates the occurrence of the chemical threshold. Since the R-value is 1.75 for the present system it suggests Se rich material having heteropolar bonds and chalcogen-chalcogen bonds. The heteropolar bonds are also more favorable than homopolar bonds due to their larger bond energies. The weak bands up to 136 cm^{-1} are reported to be of mixed character with identical contributions from Ag, Se and In atoms [21]. Therefore, the observation of weak band can be ascribed to

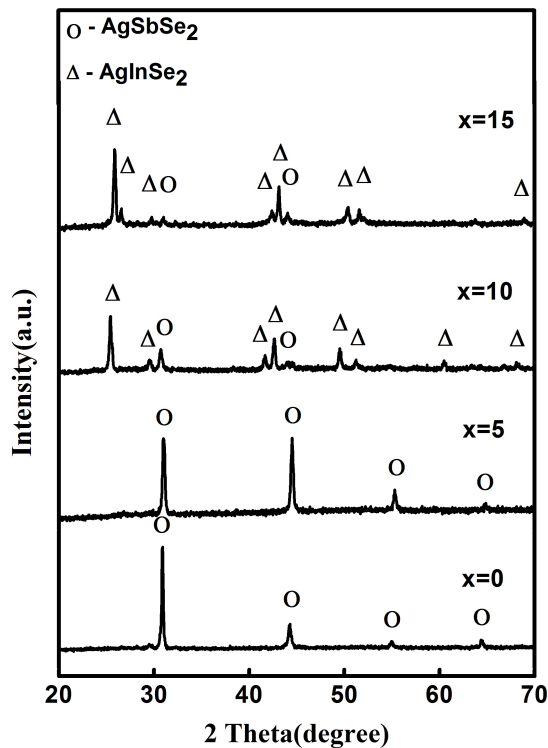


Fig. 2. X-ray diffraction patterns for $\text{In}_x\text{Sb}_{20-x}\text{Ag}_{10}\text{Se}_{70}$ chalcogenide alloys.

the contributions from Se and Ag atoms in the parent ternary system. Holubova *et al.* [22] have assigned the peak at 194 cm^{-1} to heteropolar Sb–Se bond vibrations in $\text{SbSe}_{3/2}$ pyramids so, the peak observed at 188 cm^{-1} can be ascribed to Sb–Se bond vibrations of AgSbSe_2 structural units due to the incorporation of Ag in this ternary system. However, the broadening of this peak with indium content can be ascribed to the replacement of Sb by In in AgSbSe_2 structural units. The peak at 252 cm^{-1} may correspond to the homopolar Sb–Sb bonds in $\text{Se}_2\text{Sb}-\text{Se}_2\text{Sb}$ structural units [23]. The band at 369 cm^{-1} has been ascribed to the bond bending modes of Se [24]. Therefore, the band at 371 cm^{-1} can be assigned to this mode. The observed shift may be due to the presence of Sb or Ag. This band was found to fade with the increase in the indium concentration due to breaking of Se chains.

The peak at 82 cm^{-1} has been found to broaden for all the concentrations, while the band

at 117 cm^{-1} broadens for $x = 5$ and disappears for $x = 10$ and 15 at.%. The intensity ratio for 188 cm^{-1} and 252 cm^{-1} peaks have been found to increase up to $x = 5$, and thereafter, this value decreased with the appearance of new band at 238 cm^{-1} for $x = 10$ sample. The B_2 mode of $AgInSe_2$ chalcopyrite structure has been reported at 230 cm^{-1} [25] and therefore, the shift can be ascribed to the presence of Sb atoms in this system. It has further been observed that when the In content increases ($x = 15$), the intensity for 238 cm^{-1} peak increases as compared to the intensity of 252 cm^{-1} peak, indicating a decrease of the homopolar Sb–Sb bonds and increase in the heteropolar In–Se bonds. The relative decrease in the intensity for the 252 cm^{-1} peak at higher In content can be ascribed to the segregation of $AgInSe_2$ phase. Also, the new weak band at 142 cm^{-1} can be assigned to the B_2 mode corresponding to the antiphase motion between In and Se atoms of $AgInSe_2$ chalcopyrite structure [25].

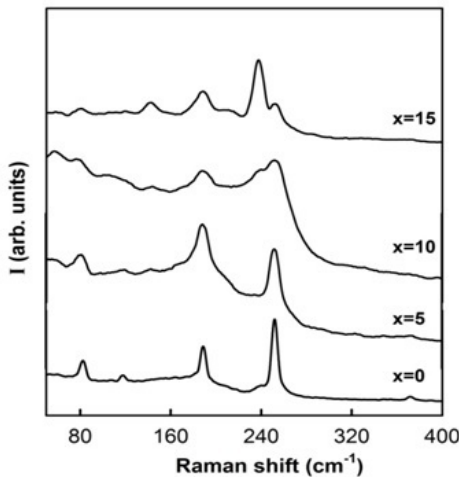


Fig. 3. Raman spectra of $In_xSb_{20-x}Ag_{10}Se_{70}$ chalcogenide alloys.

3.3. Optical spectroscopy

The relation between absorption coefficient and diffuse reflectance has been given by Kubelka-Munk [26]:

$$\alpha = \frac{k}{s} = \frac{(1-R_\infty)^2}{2R_\infty} \quad (1)$$

where s and k are the scattering and absorption coefficients. Fig. 4 shows the variation of $(\alpha h\nu)^2$ versus photon energy (E) for the present system.

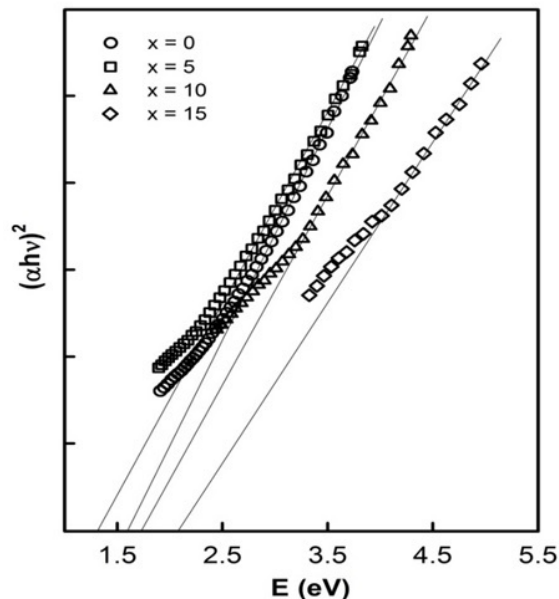


Fig. 4. The variation $(\alpha h\nu)^2$ versus photon energy (E) for bulk polycrystalline $In_xSb_{20-x}Ag_{10}Se_{70}$ chalcogenide alloys.

Table 2. Optical band gap (E_g) and tailing parameter (B^{-1}) of the as-prepared $In_xSb_{20-x}Ag_{10}Se_{70}$ chalcogenide alloys.

Composition (x)	E_g [eV]	B^{-1} $\times 10^{-4}\text{ cm}^{-1}\cdot\text{eV}^{-1}$
0	1.59	137.5
5	1.30	138.7
10	1.71	69.4
15	2.06	54.1

The band gap can also be calculated by the following equation [27]:

$$\alpha = B \frac{(h\nu - E_g)^n}{h\nu} \quad (2)$$

where B is a constant, E_g is the band gap and $n = 1/2$ corresponds to the allowed direct transitions [28]. The parameter B depends upon the transition probability, the inverse of which is known as

tailing parameter describing the disorder in the network systems [29, 30]. Fig. 4 reveals direct band transitions for $\text{In}_x\text{Sb}_{20-x}\text{Ag}_{10}\text{Se}_{70}$ alloys. The values of band gap and tailing parameter are summarized in Table 2. The value of E_g for $\text{Sb}_{20}\text{Ag}_{10}\text{Se}_{70}$ alloy is 1.59 eV and decreases to 1.30 eV for 5 at.% of indium with the increase in tailing parameter. This can be correlated with the decrease in disorder of the system. The dominant contribution for the states near the band edge of the chalcogenide alloys comes from their lone pair p-orbital [31]. The electronegativity of Sb, Ag, Se and In are 2.05, 1.93, 2.55 and 1.78 respectively [32]. When Sb atom is replaced by the electropositive In atom, the energy of lone pair of electrons gets enhanced and hence, the valence band edge moves towards the forbidden gap to cause an increase in the tailing parameter and decrease in the optical gap for this system [33]. Further addition of In have been found to increase the band gap to 1.71 and 2.06 eV for $x = 10$ and 15, respectively. This can be explained by considering the bond formation energies. For hetero-nuclear bonds, the bond energy (BE), E_{A-B} has been calculated by using the relation [34]:

$$E_{A-B} = (E_{A-A} \times E_{B-B})^{1/2} + 30(\chi_A - \chi_B)^2 \quad (3)$$

where E_{A-A} and E_{B-B} are the BE of the homo-nuclear bonds and χ_A , χ_B are the electronegativities of the atoms respectively. The calculated bond energies are Se–Se (44.02 kcal/mol), Sb–Sb (30.02 kcal/mol), In–In (24.2 kcal/mol), Sb–Se (40.15 kcal/mol), Sb–In (30.72 kcal/mol) and In–Se (47.33 kcal/mol) [35]. According to the chemically ordered network model, an atom combines preferably with the atoms of different kind as compared with the same atoms and the bonds are formed in the sequence of the BE [2]. The increase in In and decrease in Sb lead to the relative increase in AgInSe_2 phase at the expense of AgSbSe_2 phase or replacing the weaker Sb–Se and Sb–In bonds by stronger In–Se bonds in this system. Therefore, the band gap is found to decrease for lower indium concentrations where the system forms the solid solutions. Similar effects associated with the incorporation of In on the electrical properties have been observed in $\text{Se}_{90-x}\text{Te}_5\text{Sn}_5\text{In}_x$ glassy alloys [36]. The XRD studies have also revealed the increase

in the relative increase in AgInSe_2 phase at the expense of AgSbSe_2 phase as earlier discussed. This leads to an increase in the average bond energy and hence, an increase in the optical gap for this system.

4. Conclusions

Bulk samples of $\text{In}_x\text{Sb}_{20-x}\text{Ag}_{10}\text{Se}_{70}$ chalcogenides have been synthesized by conventional melt quenching technique and found to be polycrystalline with the formation of tetragonal AgSbSe_2 and AgInSe_2 phases. The composition of the bulk samples have been found to be close to those taken for the synthesis. The main Raman band at 188 cm^{-1} have been assigned to Sb–Se vibrations in the $\text{SbSe}_{3/2}$ pyramids, a basic structural unit of AgSbSe_2 phase, and the 252 cm^{-1} band for the homopolar Sb–Sb bonds in $\text{Se}_2\text{Sb}-\text{Se}_2\text{Sb}$ structural units for the $x = 0$ sample. The value of intensity ratio for 188 cm^{-1} and 252 cm^{-1} bands have been found to increase up to $x = 5$, and thereafter, this value decreased with the appearance of the new band at 238 cm^{-1} corresponding to B2 mode of AgInSe_2 chalcopyrite structure for $x = 10$ sample. The weak band at 142 cm^{-1} corresponds to antiphase motion between In and Se for the AgInSe_2 chalcopyrite structure with 15 at.% of In. The direct optical band gap has been found to decrease up to $x = 5$ and thereafter, the value was found to increase having inverse relation with the tailing parameter. The variations in the optical properties have been discussed by considering the electronegativity of the additive, change in average bond energy and the structural modifications of the network.

Acknowledgements

One of the authors (RS) is thankful to the DST, Govt. of INDIA, New Delhi [No. SR/S2/CMP- 0008/2011], for providing the financial support.

References

- [1] STUDENTYAK I.P., KUTSYK M.M., BUCHUK M.Y., RATI Y.Y., NEIMET Y.Y., IZAI V.Y., KOKENYESI S., NEMEC P., *Opt. Mater.*, 52 (2016), 224
- [2] ELLIOT S.R., *Physics of amorphous materials*, Longman Publication, London, 1991.

- [3] FRITZSCHE H., *J. Phys. Chem. Solids*, 68 (2007), 878.
- [4] PATTANAYAK P., ASHOKAN S., *Euro. Phys. Lett.*, 75 (2006), 778.
- [5] HAMANN H.F., BOYLE M.O., MARTIN Y.C., ROOKS M., WICKRAMASINGHE H.K., *Nat. Mater.*, 5 (2006), 383.
- [6] BALITSKA V., SHPOTYUK O., ALtenburg H., *J. Non-Cryst. Solids*, 352 (2006), 4809.
- [7] STRONSKI A., ACHIMOV A., PAIUK O., MESHLAKIN A., ABASHKIN V., LYTVIN O., SERGEEV S., PRISACAR A., TRIDUH G., *Nanoscale Res. Lett.*, 11 (2016), 39.
- [8] AFIFI M.A., ABD EL-WAHABB E., BEKHEET A.E., ATYIA H.E., *J. Mater. Sci.*, 41 (2006), 7969.
- [9] ZHENG W.X., XIE Y., ZHU Y.L., JIANG X.C., JIA Y.B., SUN Y.P., *Inorg. Chem.*, 41 (2002), 455.
- [10] YU Y., WANG R.H., CHEN Q., PENG L., *J. Phys. Chem. B*, 110 (2006), 13415.
- [11] ABDEL-RAHIM M.A., HAFIZ M.M., SHAMEKH A.M., *Physica B*, 369 (2005), 143.
- [12] SOLIMAN H.S., ABDEL-HADY D., IBRAHIM E., *J. Phys. Condens. Mat.*, 10 (1998), 847.
- [13] KAUR G., KOMATSU T., *J. Mater. Sci.*, 36 (2001), 4531.
- [14] WOJCIECHOWSKI K., TOBOLA J., SCHMIDT M., *J. Phys. Chem. Solids*, 69 (2010), 2748.
- [15] WANG K., STEIMER C., WUTTIG M., *J. Optoelectron. Adv. M.*, 9 (7) (2007), 2008.
- [16] AL-GHAMDI A.A., KHAN S.A., AL-HENTI S., AL-AGEL F.A., ZULFEQUAR M., *Curr. Appl. Phys.*, 11 (2011), 315.
- [17] MOTT N.F., DAVIS E.A., *Electronic Processes in Non-Crystalline Materials*, Oxford Press, Clarendon, 1979, p. 132.
- [18] BOOLCHAND P., GEORGIEB D.G., GOODMAN B., *J. Optoelectron. Adv. M.*, 3 (2001), 703.
- [19] THORPE M.F., *J. Non-Cryst. Solids*, 57 (1983), 355.
- [20] KUMAR P., THANGARAJ R., *J. Non-Cryst. Solids*, 352 (2006), 2288.
- [21] KOPYTOV A.V., KOSOBUTSKY A.V., *Phys. Solid State*, 51 (2009), 2115.
- [22] HOLUBOVA J., CERNOSEK Z., CERNOSKOVA E., *J. Optoelectron. Adv. M.*, 1 (2007), 663.
- [23] IVANOVA Z.G., CEMOSKOVA E., VASSILEV V.S., BOYCHEMA S.V., *Mater. Lett.*, 57 (2003), 1025.
- [24] OHTA N., SCHEUERMANN W., NAKAMATA K., *Solid State Commun.*, 27 (1978), 1325.
- [25] JIN Y., TANG K., AN C., HUANG L., *J. Cryst. Growth*, 253 (1–4) (2003), 429.
- [26] MARFUNIN A.S., EGOGROVA N., MISCHHENKO A., *Physics of Minerals and Inorganic Materials: An Introduction*, Springer, Berlin, 1979.
- [27] PANKOVE J.I., *Optical processes in semiconductors*, Dover Publications, New York, 1971.
- [28] KAMATSU A., TAKEI S., MIZUHATA M., *Thin Solid Films*, 359 (1) (2000), 55.
- [29] KUMAR P., THANGARAJ R., SATHIARAJ T.S., *Phys. Status Solidi A*, 208 (4) (2011), 838.
- [30] TAUC J., *Amorphous and Liquid Semiconductors*, Plenum Press, New York, 1974, p. 569.
- [31] KASTNER M., ADLER D., FRITZSCHE H., *Phys. Rev. Lett.*, 37 (1976), 1504.
- [32] PAULING L., *The Nature of Chemical Bond*, Cornell University, New York, 1976.
- [33] SHARDA S., SHARMA N., SHARMA P., SHARMA V., *Def. Diff. Forum*, 45 (2011), 316.
- [34] KATYAL S.C., VERMA R.C., *J. Phys. Condens. Mat.*, 5 (1993), 3469.
- [35] AMER H.H., ZEKRY A.E.H., EL ARABY S.M.S., GHAREEB K.E., ELSHAZLY A.A., *Arab. J. Nuc. Sci. Appl.*, 45 (3) (2012), 256.
- [36] RAM I.S., KUMAR S., SINGH R.K., SINGH P., SINGH K., *AIP Adv.*, 5 (2015), 087164.

Received 2016-02-16

Accepted 2016-09-05